Renewable and Sustainable Energy Reviews 161 (2022) 112250

Contents lists available at ScienceDirect

Renewable and Sustainable Energy Reviews

journal homepage: www.elsevier.com/locate/rser

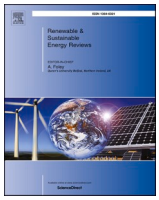

Reliability of offshore wind turbine support structures: A state-of-the-art review

L. Wang [a,*], A. Kolios [b], X. Liu [c], D. Venetsanos [d], C. Rui [e]

[a] School of Mechanical, Materials and Manufacturing Engineering, University of Nottingham, Nottingham, NG7 2RD, United Kingdom
[b] Department of Naval Architecture, Ocean & Marine Engineering, University of Strathclyde, Glasgow, G4 0LZ, United Kingdom
[c] Entrust Smart Home Microgrid Ltd, Lancaster, LA1 2TH, United Kingdom
[d] Department of Engineering and Technology, University of Huddersfield, Queensgate, Huddersfield, HD1 3DH, United Kingdom
[e] School of Mechanical, Aerospace and Automotive Engineering, Coventry University, Coventry, CV1 5FB, United Kingdom

ARTICLE INFO

Keywords:
Offshore wind turbine
Support structures
Reliability assessment
Structural reliability
Fatigue reliability

ABSTRACT

OWT (Offshore Wind Turbine) support structures are exposed to harsh ocean environment with significant uncertainties in soil properties and environmental loads. Reliability assessment of OWT support structures taking into account those uncertainties is crucial in the development of more cost-effective OWT support structures. This paper presents a state-of-the-art reliability assessment of OWT support structures, providing a comprehensive review on the structural reliability, reliability-based calibration of codes, fatigue reliability and the implementation of reliability assessment. The current and future developments of reliability assessment of OWT support structures, such as reliability-based design optimisation, multi-hazard reliability analysis and risk-based inspection, are also presented. This paper has been written for both 1) researchers new to this research area through providing a comprehensive review on the latest research and summarising underlying theory; and 2) experts in this research area through presenting a comprehensive list of relevant references where the details of analysis methods can be acquired.

1. Introduction

During the period from 2005 to 2019, wind power technology has experienced significant development with over 1100% increase in global cumulative installed wind capacity, which reached around 651 GW at the end of 2019 [1]. The wind industry is moving to offshore, as the wind in offshore locations is steadier and stronger and there are more spaces available at sea to install wind turbines when compared to the land [2]. According to WindEurope [3], the cumulative installed capacity of offshore wind power in Europe by the end of 2019 was about 22.1 GW, with a total of 5047 OWTs (Offshore Wind Turbines). Projections show that it will continuously grow, reaching 70 GW by 2030 [4].

The design of support structures for OWTs is quite different from that for onshore wind turbines. Firstly, the load conditions in offshore locations are different from those in onshore locations. In addition to the wind loads, OWT support structures are also subjected to significant hydrodynamic loads, which are not experienced by onshore wind turbines. Additionally, onshore wind turbines generally use concrete foundations, while the type of foundations used for OWTs is highly dependent on the water depth.

There are a variety of types of support structures for OWTs [5]. They can be roughly categorised into two groups: 1) bottom-fixed support structures, including gravity-base [6], monopile [7,8], caisson [9], tripod [10] and jacket [11,12]; 2) floating support structures, including spar-buoy [13,14], tension-leg platform [15,16] and barge-type [17]. The selection of the type of support structure needs to take into account multiple criteria, such as financial constraints, seabed conditions and water depth [18–22]. Gravity-base support structures are mainly used for water depths of up to 27 m [23]. Because of their ease of both fabrication and installation, monopiles are presently the most widely used foundation, representing around 70% of European Union's newly installed foundations in 2019 [3]. Monopiles were deemed to be suitable for water depth shallow than 30 m [24]; however, the water depth limits of applicability of monopiles have been shifting and monopiles have been recently applied for water depths exceeding 40 m [25,26]. Tripod structures are suitable for water depth of up to 80 m [27]. For water depths of 40–100 m, jacket structures are commonly used [28,29]. For water depths deeper than 100 m, floating support structures are deemed

* Corresponding author.
E-mail address: lin.wang1@nottingham.ac.uk (L. Wang).

https://doi.org/10.1016/j.rser.2022.112250
Received 27 April 2020; Received in revised form 11 December 2021; Accepted 6 February 2022
Available online 16 March 2022

Abbreviations

ABS	American Bureau of Shipping
ALS	Accidental Limit State
BLS	Buckling Limit State
CM	Condition Monitoring
DLS	Deflection Limit State
FEA	Finite Element Analysis
FLS	Fatigue Limit State
FORM	First Order Reliability Method
FOSM	First-Order Second-Moment
MCS	Monte Carlo Simulation
OPEX	Operating Expense
OWT	Offshore Wind Turbine
O&M	Operation and Maintenance
PISA	Pile Soil Analysis
PSF	Partial Safety Factor
RBDO	Reliability-based Design Optimisation
RBI	Risk-based Inspection
SHM	Structural Health Monitoring
SLIC	Structural Lifecycle Industry Collaboration
SLS	Serviceability Limit State
SORM	Second Order Reliability Method
ULS	Ultimate Limit State
VLS	Vibration Limit State
1D	One-dimensional
3D	Three-dimensional

Nomenclature

a	Crack size
a_0	Initial crack size
a_{cr}	Critical crack size
a_i	Regression coefficients
A	Intercept of S–N curve
A_R	A $(p \times q)$ data matrix that contains the regression coefficients
b	geometrical property
C, M	Crack propagation parameters
D	Design space
D_A	Aggregate deviation
D_F	Fatigue damage ratio
$D_{F,t}$	Fatigue damage ratio expected during the design life of a structure
D_f	Failure region of design space
D_s	Safe region of design space
d	Design values
d_{allow}	Allowable deflection
d_{max}	Maximum deflection
E	Load effect
E_{et}	A $(n \times q)$ data matrix with error terms
$E(S^m)$	Expected value of random variable S^m
E_d	Design value of load effect
F_{dj}	Design value for load j
F_{kj}	Representative value for load j
f_{ki}	Characteristic strength of material i
f_0	First natural frequency of OWT support structure
f_{1P}	Rotating rotor induced frequency
f_{3P}	Blade-passing frequency
$f_S(S_i)$	Probability density function of stress range
g	Performance function
g_u	Performance function under ultimate limit state
g_d	Performance function under deflection limit state
g_b	Performance function under buckling limit state
k	Thickness exponent on fatigue strength
ΔK	Range of stress intensity factor
L_m	Buckling load multiplier
$L_{m,min}$	Minimum acceptable load multiplier
m	Slope of S–N curve
n_b	number of different stress levels
n_i	number of loading cycles accumulated at stress range S_i
N	Number of loading cycles
N_i	average number of loading cycles to failure at stress range S_i
N_t	Number of loading cycles that the structure is expected to experience during its design life
P_f	Probability of failure
R	Resistance
R_d	Design value of resistance
S	Stress range
S_e	Equivalent stress range
t	Plate thickness
t_{ref}	Reference thickness
X	Vector containing random variables
X_I	A $(n \times p)$ data matrix that contains different powered values of independent variables
X_{di}	Design value for strength of material i
$Y(a)$	A function of crack geometry
Y_D	A $(n \times q)$ data matrix that contains the dependent variables
α_R, α_E	FORM sensitivity factors
α_i	$\beta_i \cdots, \omega_i$ Power coefficient for independent variables
β	Reliability index
β_k	reliability index for element k
β_t	target reliability index
γ_{fj}	Partial factor of load j
γ_{mi}	Partial factor of material i
σ_{allow}	allowable stress
σ_{max}	maximum von-Mises stress
σ_S	standard deviation of stress range S
ε'	Uncertainty in the S–N relationship
θ	model uncertainty
μ_S	mean of stress range S

more suitable than bottom-fixed support structures [30–33].

OWT support structures are exposed to the harsh ocean environment with significant uncertainties in soil properties and environmental loads. The traditional way to account for uncertainties is to treat them deterministically, applying a PSF (Partial Safety Factor) on loads and material properties. This simplification used in the design process generally leads to either over-sized or under-designed designs in most cases. An alternative way of treating uncertainties is the stochastic modelling, in which the uncertainties in variables are taken into account by modelling variables stochastically with appropriate types of distributions (e.g. normal, lognormal, Weibull, etc.). Stochastic modelling has been deemed as a promising way to take into account uncertainties in stochastic variables, and has been extensively applied to reliability assessment of offshore structures and renewable energy devices [34–37].

Reliability-based calibration of codes and standards provides an efficient way for adjusting PSFs to account for certain load regimes and deployment locations, ensuring adequate safety and avoiding unnecessary generalisation of generic PSFs. This practice has been widely applied over the last decade and is widely adopted from documents such as Eurocode recommended guidelines [38] and background documentations [39,40] which illustrate basic steps of the calibration process.

In addition to calibrating PSFs, structural reliability analysis is also a

key element of the probabilistic design approach. Structural reliability analysis is concerned with the prediction of the probability of limit-state violations of a structure. The formulation of limit states is based on the first principles, also known as failure modes with physics behind them. The main failure modes of OWT support structures include fatigue, buckling, scouring, cracks in welds, excessive deflection, corrosion, vibration and fouling [41,42].

OWT support structures experience significant cyclic loads, such as wind and wave loads. Their design is therefore typically dominated by fatigue reliability [43]. The fatigue analysis methods used in fatigue reliability assessment can be roughly divided into two groups: 1) S–N curve method [44], which is on the basis of S–N data typical obtained through fatigue testing; and 2) fracture mechanics method [45], which requires the use of crack growth data of an initial defect. To improve the fatigue reliability of OWT support structures, it is crucial to develop effective fatigue reliability assessment models.

So far few review papers on the reliability of wind turbines have been published. Sheng [46] conducted a survey of various databases on wind turbine subsystem reliability. The survey provided a brief summary of each database and highlighted key results that were deemed beneficial. Wen et al. [47] reviewed probabilistic methods used for assessing wind power reliability and discussed the factors that influence the reliability of wind power system. Pfaffel et al. [48] conducted a review on the performance and reliability of wind turbines. The failure rates of different wind turbine components (subsystems), including rotor, drive train system, yaw system, central hydraulic system, control system, power generation system, transmission, nacelle, cooling system, meteorological measurement and tower system, were reviewed and discussed. However, reliability of OWT support structures is not covered by these papers. To facilitate the development of more cost-effective OWT support structures, it is crucial to have a review of the state of the art in reliability assessment of OWT support structures. Due to this concern, a comprehensive review of the reliability assessment of OWT support structures has been developed in this paper.

The structure of the paper is as follows. Section 2 reviews structural reliability assessment methods. Section 3 reviews reliability-based calibration of codes and standards. Section 4 presents fatigue reliability, and Section 5 presents the implementation of reliability assessment of OWT support structures. Section 6 present current and future trends in reliability of OWT support structures, followed by conclusions in Section 7. It should be noted that the structural reliability assessment methods, reliability-based calibration of codes and fatigue reliability reviewed in this paper can be applied to any type of OWT support structure. In this paper, the procedure of the implementation of reliability assessment of OWT support structures is illustrated through the typical procedure used for bottom-fixed OWT support structures.

2. Structural reliability assessment methods

In reliability analysis, the reliability index is generally used to quantify risks and therefore assess the consequences of failure [49]. The governing parameters of the problem are generally modelled as random variables, which can be grouped in a random vector X.

For reliability analysis, the space D of random variables can be divided into two regions: failure region D_f and safety region D_s, which are defined by Eqs. (1) and (2), respectively.

$$D_f = \{X | g(X) \leq 0\} \tag{1}$$

$$D_s = \{X | g(X) > 0\} \tag{2}$$

where g is the performance function. $g(X) = 0$ denotes limit state surface, which is defined as the boundary between failure and safe regions.

In the simplest case, the performance function g is given by:

$$g = R - E \tag{3}$$

where R is the resistance, E is the load effect.

For structural reliability analysis, the performance function g is typically expressed in terms of displacement, strain, stress and modal frequency.

According to the degree of sophistication applied to deal with various problems, structural reliability analysis methods can be roughly grouped into four levels: Levels I, II, III and IV [50].

2.1. Level I methods

Level I methods, which describe each uncertain variable using only one characteristic value, are deterministic reliability methods. In those methods, probability of failure is not computed explicitly, and uncertainties in variables are taken into account by applying a set of PSFs taken from design standards. The PSFs specified in the design standard are generally commensurate with a target reliability.

2.2. Level II methods

In the Level II reliability analysis methods, two values (i.e. mean and variance) are generally used to describe each uncertain variable. Reliability index method, e.g. the FOSM (First-Order Second-Moment) method [51], is an example of Level II methods.

2.3. Level III methods

Level III reliability analysis methods describe uncertain variables using their joint probability distribution. The basic reliability measure used in these methods is the probability of failure, which corresponds to a reliability index. The approximatively analytical analysis methods, such as FORM (First Order Reliability Method) [52] and SORM (Second Order Reliability Method) [53], and simulation methods, such as directional sampling and MCS (Monte Carlo Simulation) [54], fall into this category. Level III methods generally provide reasonable results, and they are recommended by DNV standard [50].

2.4. Level IV methods

Level IV reliability methods compare a structural prospect with a reference prospect according to the principles of engineering economic analysis under uncertainty. They go beyond Level III methods by considering extra aspects, such as target reliability, maintenance and costs. They account for the consequences of failure and aim to maximise the expected cost-benefits for a structure in its expected lifetime.

2.5. Comparison of reliability analysis methods

Table 1 shows a comparison of four levels of reliability analysis methods, in terms of whether or not to use PSFs, number of characteristic values used for each stochastic variable, whether or not to use joint probability and whether or not to consider extra aspects (e.g. target reliability, costs, benefits of construction, etc.). Examples of different levels of reliability analysis methods are also presented in Table 1. Currently, Level III methods are the most widely used reliability analysis methods for OWT support structures [55,56], as they generally provide reasonable results. Level IV methods go beyond Level III methods through taking into account extra aspects (such as target reliability, maintenance and costs), and they will be increasingly used in the future.

3. Reliability-based calibration of codes and standards

Empirical and experimental knowledge of probabilistic concepts has been gained through historical development. The systematic recording of this knowledge is beneficial to develop a methodology, which allows the design of novel structures to achieve a desired level of reliability and

Table 1
Comparison of reliability analysis methods.

Level of method	PSFs used	No. of characteristic values used for each stochastic variable	Joint probability distributions used	Extra aspects considered	Examples
I	Yes	One	No	No	PSF
II	No	Two	No	No	FOSM
III	No	Two or more	Yes	No	FORM, SORM, MCS
IV	No	Two or more	Yes	Yes	Combining FORM with an optimiser to achieve target reliability, taking into account engineering costs.

can be beneficial in the composition of relevant design codes and standards. This section starts with reviewing standards used in the design of offshore structures. The design safety level and reliability-based calibration of PSFs are then presented, followed by discussing the limitations of existing design standards.

3.1. Standards for offshore structures

3.1.1. API RP-2A: recommended practice for planning, designing and constructing fixed offshore platforms – working stress design

This recommended practice, which followed the working design stress format in its initial publication, was developed by the API (American Petroleum Industry) in 1969. A draft version was issued in a Load Resistance Factor Design format in 1989, and it was publicly released in 1993 [57]. This standard is currently on its 22nd edition [58], released in November 2014.

3.1.2. BS EN 1993-1-1:2005 + A1:2014 eurocodes 3: design of steel structures

The Eurocodes are a set of standards developed by the European Commission [59]. Those standards enable a design on the basis of probabilistic approaches [60], which provides the opportunity for further design optimisation. BS EN 1993-1-1:2005 + A1:2014 [61], which refers to the design of steel structures, is applicable to the design of offshore structures.

3.1.3. IEC 61400–3:2019 wind energy generation systems – part 3: design requirements for offshore wind turbines

IEC 61400–3:2019 [62,63], which aims at providing an appropriate level of protection for OWTs against damage from all hazards throughout their designed lifetime. It is generally used in conjunction with the appropriate ISO and IEC standards, in particular with IEC 61400–1 [64]. For fixed and floating installations, references are made to IEC 61400-3-1:2019 [62] and IEC 61400-3-2:2019 [63], respectively.

3.1.4. DNV GL offshore standards

DNVGL-ST-0126 [65], the DNV GL standard for design of OWT support structures, covers the design, construction, installation and inspection of OWT support structures. It is in compliance with IEC61400-3; however, the requirement specified in DNVGL-ST-0126 in some scenarios is stricter than those in IEC61400-3. The DNV GL standard for design of floating wind turbines is presented in DNVGL-ST-0119 [66], and the standard for offshore substations is covered in DNVGL-ST-0145 [67].

3.1.5. ABS guides for building and classing Onshore/Offshore Wind Turbine installations

The ABS onshore guide [68] provides criteria for the design, fabrication, installation and survey of bottom-fixed OWT installations, while the ABS offshore guide [69] provides those criteria for floating OWTs. Both guides are developed by ABS (American Bureau of Shipping), which is a provider of classification and design guides for offshore industry.

3.1.6. Bureau Veritas rules and guidelines

Bureau Veritas is a company specialised in testing, inspection and certification founded in 1828. It has released a series of rules and guidelines (such as NI572 [70], NR445 [71] and NI631 [72]) for offshore structures. NI572 [70] provides specific recommendations and guidance for the certification and classification of floating OWTs. NR445 [71] documents the rules for the classification of offshore units, and NI631 [72] provides an overview of the certification scheme applicable to marine renewable energy technologies.

3.2. Design safety level

3.2.1. Safety class

In several standards (e.g. ISO [73], IEC [62,63] and DNV GL [65]), a safety class method is used to ensure the structural safety. According to failure consequences, the structures are classified into a safety class. For each safety class, a nominal annual probability of failure is generally used to define a target safety level.

According to DNV GL [65], there are two safety classes for OWTs, i.e. 1) normal safety class, which applies when a failure leads to risk of personal injury and/or environmental, economic or social consequences; 2) special safety class, which applies when the safety requirements are agreed between the customer and the designer and/or the safety requirements are decided by local regulations.

3.2.2. Target safety level

Table 2 summarises the values of acceptable annual probabilities of failure based on DNV Classification Note 30.6 [50], and Table 3 presents a comparative analysis of target safety levels based on different sources [74]. β_t in Table 2 represents the target reliability index.

According to DNVGL-ST-0126 [65], a nominal annual probability of failure of 10^{-4} should be taken as the target safety level for the design of OWT support structures. This target safety level reflects that OWT support structures are unmanned structures and designed to normal safety class.

Table 2
Values of acceptable annual probabilities of failure P_f [50].

Class of failure	Consequence of failure	
	Less serious	Serious
I – Redundant structure	$P_f = 10^{-3}$ ($\beta_t = 3.09$)	$P_f = 10^{-4}$ ($\beta_t = 3.71$)
II – Significant warning before the occurrence of failure in a non-redundant structure	$P_f = 10^{-4}$ ($\beta_t = 3.71$)	$P_f = 10^{-5}$ ($\beta_t = 4.26$)
III – No warning before the occurrence of failure in a non-redundant structure	$P_f = 10^{-5}$ ($\beta_t = 4.26$)	$P_f = 10^{-6}$ ($\beta_t = 4.75$)

Table 3
Comparative estimates of target P_f [74].

Source	Allowable system failure probability
Risk Analysis (analytical assessment)	10^{-6}/yr
CSA (Canadian Standards Association)	10^{-5}/yr
DNV	$10^{-6} - 10^{-5}$/yr
ISO - 1000 people	10^{-7}/yr
Professional recommendations	10^{-5} life time
Social Criteria – 1000 people	$10^{-7} - 10^{-5}$/yr
Existing Structures	$10^{-7} - 10^{-5}$/yr

3.3. Reliability-based calibration of PSFs

3.3.1. Calibration of PSFs by calibrating design values

In the reliability-based calibration of design values, all basic variables need to be defined with design values. The design is deemed to be safe if the limit states are not reached when the design values are introduced into the analysis model. This can be expressed as:

$$R_d \geq E_d \tag{4}$$

where the subscript d denotes design values; E_d and R_d are the design load effect and the corresponding resistance, respectively.

R_d and E_d in Eq. (4) are respectively given by Ref. [59]:

$$R_d = R\left\{X_{d1}, X_{d2}, \cdots, b_{d1}, b_{d2}, \cdots, \theta_{d1}, \theta_{d2,\cdots}\right\} \tag{5}$$

$$E_d = E\left\{F_{d1}, F_{d2}, \cdots, b_{d1}, b_{d2}, \cdots, \theta_{d1}, \theta_{d2,\cdots}\right\} \tag{6}$$

where X_{di} is the design value for strength of material i; F_{dj} is the design value for load j; b and θ are the geometrical property and model uncertainty, respectively.

The design values of resistances R_d and load effects E_d should be defined such that the following equations are satisfied:

$$P(R < R_d) = \Phi(-\alpha_R \beta_t) \tag{7}$$

$$P(E > E_d) = \Phi(+\alpha_E \beta_t) \tag{8}$$

where β_t is the target reliability index; α_R and α_E are the values of FORM sensitivity factors.

The design values (such as X_{di} and F_{dj}) can be derived by solving Eqs. (7) and (8). Dividing the design value of a variable by its characteristic or representative value gives the relevant PSF.

3.3.2. Calibration of PSFs with partial factor format

An alternative way of reliability-based calibration of PSFs starts with some arbitrary partial factor format and requires that the partial factors are chosen in such way that reliability of the structure is as close as possible to some selected target value.

Assume the partial factor format can be written as [75]:

$$g\left(\frac{f_{k1}}{\gamma_{m1}}, \frac{f_{k2}}{\gamma_{m2}}, \cdots, \gamma_{f_1} F_{k1}, \gamma_{f_2} F_{k2,\cdots}\right) \geq 0 \tag{9}$$

where f_{ki} and γ_{mi} are the characteristic strength and partial factor of material i, respectively; F_{kj} and γ_{f_j} are the representative value and partial factor for load j, respectively.

The next step is to define a representative set of j test elements, covering 1) types of actions; 2) types of structural dimensions; 3) types of materials; and 4) types of limit states.

For a given set of partial factors $(\gamma_{m1}, \gamma_{m2}, \cdots, \gamma_{f1}, \gamma_{f2}, \cdots)$, the set of representative structural element can be designed. Each element will then possess a certain level of reliability which will deviate more or less from the target value. With the help of the reliability index β, the aggregate deviation D_A can be expressed as:

$$D_A = \sum_{k=1}^{n} \left[\beta_k\left(\gamma_{mi}, \gamma_{fj}\right) - \beta_t\right]^2 \tag{10}$$

where β_k is the reliability index for element k as a result of a design using a set of partial factors $(\gamma_{m1}, \gamma_{m2,\cdots}, \gamma_{f1}, \gamma_{f2,} \cdots)$.

Obviously, the best set of partial factors can be obtained by minimising the aggregated deviation D_A given in Eq. (10) If not all elements are considered to be equally important, weighted factors may be applied.

3.3.3. Reliability-based calibration of PSFs for OWT support structures

Several studies have been performed on the reliability-based calibration of PSFs for OWT support structures.

John [76] performed reliability-based calibration of fatigue safety factors for OWT support structures. Results indicated that slightly larger fatigue safety factors were required if the fatigue loads on the support structure are dominated by the wave loads rather than the wind loads. Velarde et al. [77] proposed a framework for reliability-based calibration of fatigue safety factors for OWT concrete support structures and applied the framework to a typical gravity-based foundation. Results indicated that the reliability-based calibration of PSFs can potentially contribute to the cost reduction in offshore wind energy. Morató and Sriramula [78] performed reliability analysis and then calibrated PSFs on the basis of reliability. The calibrated PSFs were applied to an industry-reference turbine and support structures. The results indicated that very low probabilities of failure for most sever design cases were achieved with the reliability-based calibrated PSFs.

3.4. Limitations of standards for OWT support structures

Although acceptable reliability of OWT support structures can be generally achieved with the use of design standards, limitations of these standards arise for their applicability on special and novel structures. This is due to the fact that design standards mainly refer to specific structures, and they are generally documented in a high level that typically supplies limited background information of the methods used [79]. In this aspect, the reliability-based design method is capable of providing sufficient results for the design of the special and novel OWT support structures.

PSFs can be calculated independently through reliability-based calibration [80], which avoids undesired conservativeness imposed. Additionally, in cases of high uncertainty, the consequences of failure of OWT support structures can be lowered through combining different standards where appropriate, providing a reliable design.

During the manufacturing and operation of the structure, safety elements such as quality control, condition monitoring and inspection can be used. Such practices supply additional information about the structure, reducing the overall uncertainty. With the use of condition monitoring system, it is possible to update the reliability of the structure based on the condition monitoring data. However, there is limited information provided in the existing design standards on how to integrate condition monitoring data with reliability analysis for OWT support structures.

4. Fatigue reliability

OWT support structures experience significant cyclic wind and wave loads, and their design is mainly dominated by fatigue [81–83]. Their reliability requirement is affected by their service period (typically 20 years [65]) and the inspection intervals.

4.1. Fatigue analysis method

The technical methods for fatigue analysis can be roughly classified into two groups: fracture mechanics method and S–N curve method.

4.1.1. Fracture mechanics method

The fracture mechanics method uses the crack growth data of an initial defect of assumed (or known) geometry and size. It requires the evaluation of crack growth and the calculation of the number of loading cycles that are required for initial defects to develop into cracks big enough to trigger fracture [84]. Factors that affects the fatigue crack growth in marine environment is reviewed in Ref. [85]. The crack growth is governed by the following expression:

$$\frac{da}{dN} = C\Delta K^M \tag{11}$$

where a is the crack size; N is the number of loading cycles; C and M are empirically derived crack propagation parameters; ΔK is the range of stress intensity factor.

ΔK in Eq. (11) is given by Ref. [86]:

$$\Delta K = SY(a)\sqrt{\pi a} \tag{12}$$

where S is the stress range and $Y(a)$ is a function of crack geometry.

Failure occurs when the crack size a reaches the critical crack size a_{cr}. By rearranging Eq. (11), the number of loading cycles N can be expressed as:

$$N = \frac{1}{CS^M}\int_{a_0}^{a_{cr}} \frac{da}{Y^M(a)(\sqrt{\pi a})^M} \tag{13}$$

where a_0 is the initial crack size.

The crack propagation parameters M and C in Eq. (13) depend on material types, environment and whether or not to use corrosion protection. The typical values of M and C for offshore welded steels are listed in Table 4, taken from DNVGL-ST-0126 [65].

4.1.2. S–N curve method

The S–N curve method requires the use of fatigue test data (i.e. S–N data), and the S–N curves are generally depicted as straight lines on a log-log plot [84]. The fundamental equation of S–N curve is given by:

$$N = \frac{A}{S^m} \tag{14}$$

where A and m are the intercept and slope of S–N curve in the log-log plot, respectively. Eq. (14) can also be rearranged into the following linear form [84]:

$$\log N = A - m\log S \tag{15}$$

where log is to base 10.

Given S–N data (i.e. a set of N and S) obtained from fatigue tests, a statistical analysis method (such as least-square method [87] and maximum likelihood method [88,89]) is generally used for analysing the S–N data to produce S–N curves and associated parameters (i.e. intercept A and slope m).

OWT support structures are generally made from steel plates, which are rolled and then connected together through welded joints. The plate thickness can affect the fatigue strength of welded joints. According to DNVGL-RPC-203 [90], this effect can be taken into account by a correction on stress ranges. The design S–N curve taking into account thickness effects can be expressed as [84]:

Table 4
Crack propagation parameters [65].

Condition	M	C
Welds in air and in seawater with adequate corrosion protection	3.1	$1.1e^{-13}$
Welds subjected to seawater without corrosion protection	3.5	$3.4e^{-14}$

$$\log N = A - m\log\left(S\left(\frac{t}{t_{ref}}\right)^k\right) \tag{16}$$

where t is the plate thickness, and $t = t_{ref}$ is used when the plate thickness is less than t_{ref}; t_{ref} is the reference thickness that is typically equal to 25 mm for welded connections other than tubular joints; k is the thickness exponent on fatigue strength.

The parameters involved in the S–N curve, i.e. intercept A, slope m, and thickness exponent k, depend on the material types, environmental conditions, whether or not to use cathodic protection. DNVGL C1 and D curves [90] have been widely used in the design of OWT support structures [91,92], and they are taken as examples here. The S–N curves in air, in seawater with cathodic protection and in seawater for free corrosion are presented in Table 5.

It is worth mentioning that the offshore wind industry is relatively new. Oil & Gas standards were largely migrated across and served as the basis for the creation of offshore wind standards. Much of the original research (e.g. the research behind the recommended S–N curve) is now several decades old. It was based on characteristics that were representative of typical offshore structures used in Oil & Gas industry, which fundamentally differ from typical offshore wind structures in terms of load regimes, environment and structural characteristics. In order to develop new design standards for the design and operation of OWT support structures, SLIC (Structural Lifecycle Industry Collaboration) project [93] has been carried. SLIC is a £3 m Joint Industry Project (JIP) led by Cranfield University with the participation of leading certification body DNV GL, The Department of Energy and Climate Change, The Crown Estate in the UK, and 11 Offshore Wind Operators (i.e. Centrica Renewables, DONG Energy, EDF Energy, Energie Baden-Württemberg, E. ON UK, RWE, SSE, Statkraft, Statoil, Vattenfall and Siemens). The SLIC project was created to gain an improved understanding of fatigue in butt-welded thick steel plates used in the fabrication of OWT monopile foundations. During the SLIC project, a large number of large-scale fatigue tests were performed for offshore welded structures. The fatigue test results are valuable to derive new S–N curve, which can be employed in the design of OWT support structures.

4.2. Miner's rule and equivalent stress range

Miner's rule [94], which is based on the linear damage hypothesis, has been extensively used as a cumulative damage model for fatigue failures. According to it, the fatigue damage ratio D_F is given by:

$$D_F = \sum_{i=1}^{n_b} \frac{n_i}{N_i} \tag{17}$$

where n_b is the number of different stress levels, n_i is the number of loading cycles accumulated at stress S_i, N_i is the average number of loading cycles to failure at stress S_i. Failure occurs when the fatigue damage ratio D_F reaches 1.0.

Service loadings in the majority of OWT support structures are random variables, resulting in random stress ranges which are generally described by a probability density function $f_S(S_i)$. To utilise the S–N curve, which is based on the assumption of constant amplitude stress cycles, it is crucial to establish a relationship between constant amplitude stress of the S–N curve and the characteristic value of the wind- or wave-induced random stress. This can be achieved by using an equivalent stress range S_e, which is generally determined through the application of Miner's rule. The random stress distribution can be divided into a number of stress blocks with a width of ΔS.The fractional number of cycles in each block is $f_S(S_i)\Delta S$. If N denotes the total number of cycles in the service life of OWT support structures, the number of cycles in the stress block can be expressed as [84]:

$$n_i = Nf_S(S_i)\Delta S \tag{18}$$

Table 5
C1 and D S–N curves [90].

S–N curve	Environment											
	In air					In seawater with cathodic protection					In seawater for free corrosion	
	$N \le 10^7$		$N > 10^7$		k	$N \le 10^7$		$N > 10^7$		k	A For all cycles $m = 3.0$	k
	m_1	A_1	m_2	A_2		m_1	A_1	m_2	A_2			
C1	3.0	12.449	5.0	16.081	0.15	3.0	12.049	5.0	16.081	0.15	11.972	0.15
D	3.0	12.164	5.0	15.606	0.20	3.0	11.764	5.0	15.606	0.20	11.687	0.20

Substituting Eqs. (18) and (14) into Eq. (17) yields:

$$D_F = \sum_{i=1}^{n_b} \frac{N f_S(S_i) \Delta S}{\frac{A}{S_i^m}} \tag{19}$$

As ΔS approaches to zero, Eq. (19) can be rewritten as the following integral form:

$$D_F = \frac{N}{A} \int_0^\infty S^m f_s(S) ds \tag{20}$$

The integral expression in Eq. (20) is the expected value, $E(S^m)$, of the random variable S^m. Thus, the damage ratio D_F can be expressed as:

$$D_F = \frac{N}{A} E(S^m) \tag{21}$$

$E(S^m)$ in Eq. (21) is given by:

$$E(S^m) = \int_0^\infty S^m f_S(S) dS \tag{22}$$

The expected $E(S^m)$ is relatively easy to obtain with a given distribution. The typical distribution types of stochastic variables for offshore structures is presented in Table 6 under Section 6.2. Lognormal distribution is one of the important distribution types for structural design. This is due to the fact that 1) it is appropriate for random quantities representing the sum and product of independent random variables; and 2) it is one of the commonly used probability density distributions [95]. Taking the lognormal distribution as an example, the $E(S^m)$ is given by:

$$E(S^m) = \mu_S^m \exp\left[\frac{1}{2}(m^2 - m) \ln\left(\frac{\sigma_S^2}{\mu_S^2} + 1\right)\right] \tag{23}$$

where μ_S and σ_S are the mean and standard deviation of the stress variable S, respectively.

Combining Eqs. (14) and (21) yields the equivalent stress range S_e:

$$S_e = \sqrt[m]{\frac{1}{D_F} E(S^m)} \tag{24}$$

4.3. Cycle counting methods for variable amplitude fatigue cycles

OWT support structures are generally subjected to complex environmental loads with variable amplitude. To determine the number of cycles from a variable-amplitude loading history, it requires a cycle counting method. Several cycle counting methods have been proposed, including simple-range counting, level-crossing counting, peak counting, mean-crossing-peak counting and rainflow counting [96].

In the simple-range counting method, the strain (or stress) range between successive reversals is recorded, and each range forms one-half cycle. In the level-crossing counting method, a count is recorded each time when the predetermined strain levels are crossed by the strain history. It should be noticed that 1) on the negative side of the datum, only negative crossings with a negative slope are counted; 2) on the positive side of the datum, only crossings with a positive slope are counted. The counts are then combined to form complete cycles. The largest possible cycle is formed first and then the second largest cycle from the remaining counts is formed next, and so on, until all counts have been utilised. In the peak counting method, all peak (maximum) and valley (minimum) strains in the strain-time history are counted. In this method, the peaks and valleys on the negative and positive sides of the datum are ignored, respectively. Complete cycles are then formed by combining the counts. The largest peak with the largest valley is combined first and then the second largest peak with the second largest valley is combined next, and so on, until all counts have been utilised. In the mean-crossing-peak counting method, which is a variation of the peak counting method, only the largest valley and peak between successive crossings of the mean (zero) axis are counted. A cycle is formed through combing the largest peak and valley for each crossing.

The rainflow counting method is a variation of the simple-range counting method. In this method, the strain time history is rotated so that the abscissa is vertical, with the time increasing along the downward direction. An imaginary raindrop begins at the inside tip of each valley or peak, and it flows down the sloped "roof". The raindrop falls until 1) it reaches the path of another raindrop that starts from a higher valley or peak; or 2) it comes to the opposite valley or peak that is greater than the one where it starts. Each raindrop is counted as a half cycle. The difference between the strain at the starting point of a

Table 6
Typical distribution types of stochastic variables for offshore structures [50].

Stochastic variable		Distribution type
Wave	Short-term instantaneous surface elevation (deep water)	Normal
	Short-term heights	Rayleigh
	Wave period	Longuet-Higgins
	Long-term significant wave height	Weibull
	Long-term mean zero upcrossing or peak period	Log-normal
	Joint significant height/mean zero upcrossing or peak period	3-parameter Weibull (height)/Log-normal period condition on height
	Yearly extreme height	Gumbel
Wind	Short-term instantaneous gust speed	Normal
	Long-term n-minute average speed	Weibull
	Yearly extreme speed	Gumbel
Current	Long-term speed	Weibull
	Yearly extreme speed	Gumbel
Steel properties	Yield strength	Log-normal
	Young's modulus	Normal

raindrop and the strain at the termination point is used as the strain range for a half cycle. The half cycles of the same strain ranges with opposite flow direction are combined to form complete cycles.

It should be noticed that different counting methods produce different results for the same strain-time history. When compared to other counting methods, the rainflow counting method has demonstrated good agreement with measured fatigue lives [97,98], making it the most common counting method used in the offshore structure design [99–101].

4.4. Performance functions for fatigue reliability

The initial step in the reliability-based design procedures is generally to define performance functions, which correspond to limit states for considered failure modes. The performance functions used for fatigue reliability analysis can be written as two forms: life cycle formulation and fatigue damage formulation, which are presented below.

4.4.1. Life cycle formulation

The performance function for fatigue reliability analysis in the life cycle formulation is given by either Eq. (25) or Eq. (26):

$$g_1 = N - N_t \tag{25}$$

$$g_2 = \log(N) - \log(N_t) \tag{26}$$

where g_1 and g_2 are performance functions; N_t is the number of loading cycles that the structure is expected to experience during its design life.

4.4.2. Fatigue damage ratio formulation

The performance function for fatigue reliability analysis in the fatigue damage ratio formulation is given by:

$$g = D_F - D_{F,t} \tag{27}$$

where $D_{F,t}$ is the fatigue damage ratio expected during the design life of a structure.

4.5. Generic procedure of fatigue reliability analysis of OWT support structures

A generic procedure of fatigue reliability analysis of OWT structures is presented below.

1. Generate stress range spectra.
2. Calculate the mean of the equivalent stress range based on the generated stress range spectra.
3. Choose a target reliability index β_t and design life (e.g. 20 years).
4. Define probabilistic characteristics of fatigue variables in the performance function.
5. Having identified and determined all the variables in Steps 1 to 4, reliability methods such as FORM and SORM can be then used to calculate the reliability index β.

The reliability index β acquired in Step 5 is then compared against the target reliability index β_t. If β is greater than or equal to β_t, it indicates that the structure meets fatigue reliability requirement; otherwise, the structure will likely experience fatigue failure.

4.6. Fatigue reliability assessment of OWT support structures

Studies have been performed for fatigue reliability assessment of OWT support structures. Velarde et al. [102] performed the fatigue reliability analysis of OWT monopile support structures. The results indicated that the wave-induced fatigue loads can significantly contribute to the fatigue damage of large monopiles. Dong et al. [81] performed fatigue reliability analysis of OWT jacket support structures considering the effect of inspection and corrosion. The fatigue reliability analysis was based on fracture mechanics taking into account corrosion-induced crack growth rate, and the effects of inspection were also quantified. Colone et al. [103] studied the impact of wave loads and turbulence on the fatigue reliability assessment of OWT monopile support structures. Results indicated that a lower equivalent turbulence percentile could lead to a less conservative estimation of fatigue loads. Horn and Leira [104] performed fatigue reliability analysis of OWT on a monopile support structure with stochastic availability. Results indicated that treating the availability of an OWT as a stochastic variable could increase the operational lifetime and reduce the failure probability. Shittu et al. [105] developed a fatigue reliability assessment model for OWT support structures subjected to pitting corrosion-fatigue, and applied the model to a jacket support structure. Results showed that the aspect ratio of pits at critical size could significantly affect the reliability of the structure.

5. Implementation of reliability assessment of OWT support structures

Reliability assessment of OWT support structures generally starts with defining limit states, such as fatigue and ultimate limit states. A structural model, which takes account of stochastic variables and soil-structure interactions, is required to predict the structural responses of OWT support structures subjected to complex loadings and soil-structure interactions. The results from the stochastic structural analysis are then post-processed using multivariate regression, obtaining the performance function for each limit state. The obtained performance function can be then used as input for the FORM, SORM or MCS to compute the reliability index. A typical flowchart of the reliability assessment of OWT support structures [106], proposed by the authors, is depicted in Fig. 1.

5.1. Limit states

The main failure modes of OWT support structure include plastic collapse, fatigue, excessive deflection, excessive vibration and buckling. Limit states are conditions of potential failures. According to DNV GL design standard [65], four types of limit states need to be taken into account in the design of OWT support structures, i.e. ULS (Ultimate Limit State), FLS (Fatigue Limit State), SLS (Serviceability Limit State) and ALS (Accidental Limit State).

5.1.1. ULS (ultimate limit state)

The ULS defines the capability of the structure to resist plastic collapse. The performance function under ULS, g_u, is given by:

$$g_u = \sigma_{allow} - \sigma_{max} \tag{28}$$

where $\boldsymbol{\sigma_{allow}}$ is the allowable stress, $\boldsymbol{\sigma_{max}}$ is the maximum von-Mises stress

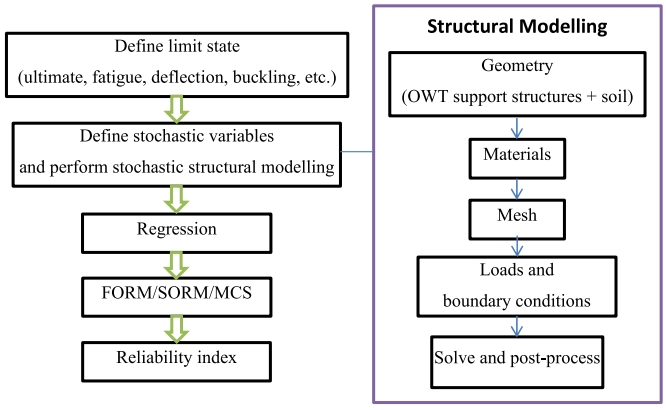

Fig. 1. Typical flowchart of reliability assessment of OWT support structures.

within OWT support structure.

5.1.2. FLS (Fatigue Limit State)

The FLS is significant in structures subjected to considerably cyclic loads, and therefore the design of OWT support structures is generally dominated by the FLS. The detailed discussion on fatigue reliability is presented in Section 4, and the performance function of FLS can be found in Section 4.3.

5.1.3. SLS (Serviceability Limit State)

SLS identifies a structure that fails to meet technical requirement for service or use. When a structure fails serviceability, it generally means that it has exceeded a limit of one of the following three aspects: 1) excessive deflection; 2) excessive vibration; and 3) excessive local deformation (buckling) [65]. Therefore, SLS can be further grouped into three limit states: DLS (Deflection Limit State), VLS (Vibration Limit State) and BLS (Buckling Limit State).

5.1.3.1. DLS (Deflection Limit State). Excessive deflections should be avoided, as they can significantly affect the serviceability of OWT support structures. The performance function under DLS, g_d, is given by:

$$g_d = d_{allow} - d_{max} \tag{29}$$

where $\boldsymbol{d_{allow}}$ is the allowable deflection, $\boldsymbol{d_{max}}$ is the maximum deflection.

Eq. (29) implies if the maximum deflection $\boldsymbol{d_{max}}$ exceeds the allowable deflection $\boldsymbol{d_{allow}}$, failure occurs.

5.1.3.2. VLS (Vibration Limit State). Vibrations induced by resonance should be considered in the design of OWT support structures. In order to avoid resonance, the first natural frequency of the OWT support structure, f_0, needs to be adequately separated from the rotating rotor induced frequency f_{1P} and blade-passing frequency f_{3P}. Currently, the most economical and common design for OWT support structures is the soft-stiff structure design [107,108], i.e. the design having first natural frequency lying between the f_{1P} and f_{3P} frequencies. According to DNV GL standard [65], a tolerance of ±5% should be applied to both the upper and lower bounds of the frequency, which can be expressed as:

$$f_{1P+5\%} \leq f_0 \leq f_{3P-5\%} \tag{30}$$

5.1.3.3. BLS (buckling limit state). OWT support structures are generally thin-walled structures and can be prone to buckling failure. Therefore, it is important to take into account of buckling in the design of OWT support structures. The performance function under BLS is given by Ref. [109]:

$$g_b(x) = L_m - L_{m,min} \tag{31}$$

where subscript $\boldsymbol{b}$ denotes the buckling limit state; $\boldsymbol{L_m}$ is the buckling load multiplier, which is defined as the ratio of the critical buckling load to the applied load on the OWT support structure; $\boldsymbol{L_{m,min}}$ is the minimum acceptable load multiplier.

Eq. (31) implies if the buckling load multiplier $\boldsymbol{L_m}$ is less than the minimum acceptable load multiplier $\boldsymbol{L_{m,min}}$, buckling failure occurs.

5.1.4. ALS (Accidental Limit State)

The ALS corresponds to 1) maximum load-carrying capacity for (rare) accidental loads; or 2) post-accidental integrity for damaged OWT support structures. The accidental loads are loads relevant to undesigned operations or technical failure, e.g. earthquake, fire, collision impact, explosions, etc. Relevant accidental loads should be determined based on an assessment and relevant experiences. More details about the ALS can be found in Ref. [65].

5.2. Structural modelling and soil-structure interactions

Assessing the structural reliability of OWT support structures needs a structural model to predict the structural responses of OWT support structures subjected to complex loading and soil-structure interaction. The structural models used for OWT support structures can be roughly classified into two groups: 1) 1D (one-dimensional) beam model, in which OWT support structures are represented using beam elements; and 2) 3D (three-dimensional) FEA (Finite Element Analysis) model, in which OWT support structures are typically modelled using shell elements. The 1D beam model is efficient in terms of computational time and capable of providing reasonable results for global responses, such as frequencies and deflections. However, it is incapable of accurately capturing local behaviour, such as local stress concentration. Comparing to the 1D beam model, the 3D FEA model requires more computational resources but it also provide more accurate results. Due to its high fidelity, the 3D FEA model has been widely applied to wind turbine structures, such as blades [110] and support structures [109].

Part of the OWT support structure (i.e. the foundation) is embedded into the soil, and the soil-structure interaction can significantly affect the structural behaviour of OWT support structures. Therefore, to accurately predict the structural responses of OWT support structures, it is crucial to take into account soil-structure interactions.

The methods for modelling soils can be roughly classified into two groups: 1) p-y method; and 2) FEA. In the p-y method, the soil is represented using distributed equivalent springs of which stiffness are derived based on the p-y curve [58]. Due to its computational efficiency, the p-y method has been widely used in the reliability analysis of OWT support structures to model the soil [55,111]. However, it was originally developed for pipes used in oil and gas industry and incapable of accurately capturing the soil behaviour of OWT support structures, of which diameters are much larger than the diameters of pipes used in oil and gas industry. In order to accurately capture the soil behaviour, it is necessary to model the soil using FEA. In the FEA model, the soil is generally modelled using 3D brick elements, and the material model for the soil is generally based on Drucker-Prager model [112] or Mohr-Coulomb model [113]. The comparison of the p-y method and FEA model was carried out in the PISA (Pile Soil Analysis) project [114–117], which is a research project led by University of Oxford. In the PISA project, experimental tests on monopiles were performed, and the results from both p-y method and FEA model were compared against experimental testing data. It is found that results from the FEA model match well with experimental data while results from p-y curve show significant discrepancy from experimental measurements. Due to its high fidelity, the FEA model has been increasingly used for modelling the soil [109,118–120].

When performing soil-structure interaction modelling, it is recommended to consider the scouring phenomena around the foundation. The scour refers to a localised loss of the soil, and it is the result of the erosion of the seabed around the foundation caused by the waves and currents. When modelling the soil using the p-y curve method, the scour can be taken into account by removing the relevant springs [121]. When modelling the soil using the FEA, the scour can be accounted for by changing the geometrical shape of the soil around the foundation [122]. Studies have shown that the scour can affect the stiffness, natural frequency and fatigue reliability of OWT support structures [123,124].

Currently, soil-structure interactions are deemed important in the design of bottom-fixed OWT support structures. The soil modelling methods reviewed in this paper are applicable to any types of the bottom-fixed OWT support structures. The main difference regarding the reliability analysis of different types of support structure is the structural modelling, as different types of support structures have different geometry and loading conditions. For floating OWT structure structures, the effects of the soil-structure interaction (e.g. the interaction among the mooring lines, the anchors and the seabed) on the design of the floating OWT support structures are yet to be explored.

5.3. Multivariate regression and reliability analysis

The relationship between a dependent variable and multiple independent variables can be established using multivariate regression. In cases of multiple independent variables, the basic equation can be solved providing sufficient sets of (y, x_i). The general problem can be expressed as:

$$y(x) = \sum_i \mathrm{a}_i p_i(x_1, x_2, \cdots, x_n) + e \tag{32}$$

Considering mononinals, this can also be described as:

$$y(x) = \sum_i \mathrm{a}_i x_1^{\alpha_i} x_2^{\beta_i} \cdots x_n^{\omega_i} + e \tag{33}$$

where $\mathrm{a_i}$ are the regression coefficients to be computed; α_i, β_i, $\cdots$, ω_i are the power coefficient for the independent variables.

In cases of second-order polynomial with two independent variables, the expression can be rewritten as:

$$y(x) = \mathrm{a}_0 + \mathrm{a}_1 x_1 + \mathrm{a}_2 x_2 + \mathrm{a}_3 x_1^2 + \mathrm{a}_4 x_2^2 + \mathrm{a}_5 x_1 x_2 + e \tag{34}$$

Eq. (33) can be also rewritten as:

$$Y_D = X_I A_R + E_{et} \tag{35}$$

where Y_D is a $(n \times q)$ data matrix that contains the dependent variables; X_I is a $(n \times p)$ data matrix that contains different powered values of independent variables; A_R is a $(p \times q)$ data matrix that contains the regression coefficients; and E_{et} is a $(n \times q)$ data matrix with error terms.

The regression coefficients A_R in Eq. (35) can be then calculated using the method of least squares:

$$A_R = \left(X_I^T X_I\right)^{-1} X_I^T Y_D \tag{36}$$

Having obtained the performance function form multivariate regression, Level III reliability analysis methods, such as FORM [52], SORM [53] and MCS [54], can be then employed to compute the reliability index.

5.4. Relevant studies on reliability assessment of OWT support structures

5.4.1. Reliability assessment of bottom-fixed OWT support structures

Studies have been performed on the reliability assessment of bottom-fixed OWT support structures. Joey et al. [125] performed fatigue reliability assessment of concrete gravity based foundation for OWTs. The fatigue damage is calculated using Miner's rule based on S–N curve method, and the reliability index is evaluated using the FORM. Results indicated that the assumption on Miner's rule uncertain has a significant influence on the fatigue reliability. Vahdatirad et al. [126] performed reliability analysis of a gravity-based foundation based on a probabilistic finite element model and the Monte Carlo simulation. The reliability analysis results then were used to calibrate a deterministic code-based design procedure. Velarde et al. [102] performed the fatigue reliability analysis of OWT monopile support structures. The results indicated that the wave-induced fatigue loads can significantly contribute to the fatigue damage of large monopiles. Colone et al. [103] studied the impact of wave loads and turbulence on the fatigue reliability assessment of OWT monopile support structures. Results indicated that a lower equivalent turbulence percentile could lead to a less conservative estimation of fatigue loads. Horn and Leira [104] performed fatigue reliability analysis of OWT on a monopile support structure with stochastic availability. Results indicated that treating the availability of an OWT as a stochastic variable could increase the operational lifetime and reduce the failure probability. Dong et al. [81] performed fatigue reliability analysis of OWT jacket support structures considering the effect of inspection and corrosion. The fatigue reliability analysis was based on fracture mechanics taking into account corrosion-induced crack growth rate, and the effects of inspection were also quantified. Shittu et al. [105] developed a fatigue reliability assessment model for OWT support structures subjected to pitting corrosion-fatigue, and applied the model to a jacket support structure. Results showed that the aspect ratio of pits at critical size could significantly affect the reliability of the structure.

5.4.2. Reliability assessment of floating OWT support structures

Currently, limited studies on the reliability assessment of floating OWT support structures can be found in the literature, as floating OWT support structures are still in their early stage of the development. Okpokparoro and Sriramula [127] proposed a reliability assessment framework through combining a FEA model and a Kriging surrogate model, and applied the framework to assess the structural reliability of OC3 Hywind Spar floating wind turbine support structure. Results indicated that the floating wind turbine support structures can be designed at consistent reliability levels using the proposed framework. More studies on the reliability assessment of floating OWT support structures would be seen in the future.

6. Current and future trends

Reliability has become increasingly important in the design of OWT support structures. The following aspects are current research focus and will be considered more frequently in future reliability research of OWT support structures.

6.1. Incorporating SHM/CM with reliability

The problem of optimising the capital expenditure to operating expense ratio is an issue with high priority for the offshore wind industry, needing cost reduction activities to ensure safety and serviceability performance. By gathering and interpreting information from OWT support structures, it becomes possible to assess safety levels of the structures through probabilistic approaches, allowing optimisation of maintenance strategies and facilitate planning for critical repairs and retrofits. Advanced monitoring systems are now available at a lower cost, allowing collection of loading and loading effects as well as structural response data. SHM (Structural Health Monitoring) and CM (Condition Monitoring) systems are designed to monitor such information over a relatively long service period in order to distinguish anomalies, detect degradation and identify damage [128]. A comprehensive review on health monitoring systems and operational safety evaluation techniques of OWTs can be found in Ref. [129].

SHM-integrated reliability assessment has been extensively used in civil engineering structures, such as bridges and buildings. Lee and Cho [130] proposed a probabilistic approach for predicting fatigue life for bridges using finite element model updating on the basis of SHM data, and applied the approach to a bridge to update its fatigue reliability index. The results indicate that the fatigue life of the bridge determined form the updated model, which is based on its present condition using the SHM data, is much longer than the fatigue life determined form the initial FEA model. Li et al. [131] developed a SHM-based reliability assessment framework for long-span cable-stayed bridges. When the bridges are equipped with the SHM system, the inputs (vehicle and environmental loads) and outputs (structural responses) of the bridge system can be collected through the monitored data. The responses of the bridge can be then used to calibrate and update the initial FEA model, obtaining the update model to evaluate the updated load effects. Having obtained the updated resistance results and load effects, the reliability assessment of the bridge can be conducted, providing valuable information for the decision-making process of bridge maintenance.

Authors [132] proposed an advanced reliability assessment model of OWT monopiles by integrating the reliability analysis method with SHM/CM technology. The SHM/CM data (such as monitored strain/-stress and crack depth) during the operation of OWT monopiles were used to reassess and update the reliability of monopile structures. The updated reliability index provides information that is valuable for

decision making on maintenance and inspection of OWT monopiles. More studies on incorporating SHM/CM with reliability for OWT support structures would be seen in the future.

To achieve the real-time evaluation of the reliability of OWT support structures based on SHM/CM techniques, it requires an accurate virtual representation of the OWT support structure (also called digital twin) and a constant flow of the data. The digital twin could either collect data, measured by SHM/CM systems, continuously or by intervals. Collecting data continuously may lead to excessive data [133]. Additionally, implementing sensors on the entire OWT support structures is unpractical and expensive. The critical locations where the sensors should be installed can be identified through FEA [134]. It should be noticed that the input parameters for the reliability analysis in some cases can be indirectly calculated through proxies, i.e. measuring a parameter and then correlating it with the required input that cannot be measured directly.

The current maintenance of wind turbines is often 1) reactive, with maintenance actions taking place after faults or failures occur (too late); or 2) preventive, with maintenance regularly performed to decrease the probability of failure (too early). The reactive maintenance generally results in significant unscheduled repairs, which take wind turbines offline costing the wind farm operators significant loss of energy revenues. The preventive maintenance often leads to unnecessary maintenance, as maintenance activities are performed regularly on the basis of calendar time regardless the condition of the wind turbine. To reduce the maintenance cost of wind turbines, an intelligent predictive maintenance framework is needed. Artificial intelligent methods, such as Artificial Neural Networks [135] and Support Vector Machine Algorithm [136], can be used to process the SHM/CM data. The processed SHM/CM data can be then integrated with the reliability analysis method to develop an intelligent predictive maintenance framework, which allows real-time evaluation of reliability of wind turbine components based on SHM/CM data and intelligently predicting potential damages and scheduling maintenance in advance.

6.2. Define the distribution types and quantify the mean and standard deviations for stochastic variables

In the reliability assessment of OWT support structures, the stochastic variables, such as soil properties and environmental loads, need to be modelled stochastically with proper distributions types and characteristics (e.g. standard deviations and mean for normal distribution). The distribution types and characteristic values of stochastic variables can significantly affect the reliability assessment results. The typical distribution types of stochastic variable for offshore structure are presented in Table 6, taken from DNV standard [50].

In order to obtain accurate reliability assessment results, it is important to define the distribution types, and quantify the mean and standard deviations. The data obtained through SHM/CM systems are valuable to define distribution types and quantify mean and standard deviations. More studies on applying SHM/CM system to quantify the properties of stochastic variables are expected to be carried out in the future.

6.3. RBDO (reliability-based design optimisation)

The reliability assessment method of OWT support structures can be further integrated with an optimiser (e.g. genetic algorithm) to perform RBDO. The target of the RBDO is to optimise OWT support structures to meet target reliability index subjected to multiple criteria/constraints. The target reliability index for OWT support structure is generally 3.72, which corresponds to a probability of failure of 10^{-4} [65].

Lee et al. [137] proposed a RBDO method for a OWT monopile transition piece. In the study, Deterministic Optimisation was firstly used to minimize the mass of a conical monopile connection, and then RBDO is used to further optimise the structure to achieve desired reliability with minimum mass. The results show that 1) the structural design of the monopile transition piece is dominated by the FLS; and 2) RBDO is valuable in shortening the design cycle and enhancing the reliability of the OWT monopile transition pieces. Yang et al. [138] proposed a RBDO model for the OWT tripod sub-structure taking into account dynamic response requirements. The dynamic response of the structure in time domain were originally predicted using a finite element model and then represented using an approximate model. The approximate model was then used during the optimisation process to achieve the optimal design taking into account uncertainties. The reliability of the structure was evaluated through Monte Carlo simulations. The results indicate that the proposed dynamic RBDO model of OWT tripod substructure is more rational and practical when comparing with the deterministic optimisation. More studies on applying RBDO to OWT support structures can be found in Refs. [139–141]. The application of RBDO to floating support structures is yet to be explored.

6.4. Multi-hazard reliability analysis of OWTs

OWTs installed in many regions are subject to multiple environmental hazards, such as typhoons and earthquakes.

Typhoons have threatened the safety of offshore wind farms in many countries (such as California and China), and failure incidents of OWTs caused by typhoons are constantly reported. The offshore wind farm of Guangdong Honghaiwan in south China was hit by Typhoon Usagi in 2013, with 17 out of 25 wind turbines knocked out causing nearly £11.6 m loss to the wind farm. In 2003, the wind farm was severely hit by a similar typhoon, with 13 out of 25 wind turbines damaged [142]. The offshore wind farm of Hainan Wenchang in south China was hit by Typhoon Rammasun in 2014, with two blades damaged and one tower collapsed. The Typhoon Rammasun also hit Guangdong Xuwen (south China) offshore wind farm, with 15 blades damaged as well as 13 towers collapsed and foundations overturned [143].

Additionally, many regions in the world, such as eastern coast of Japan and China, are prone to suffer earthquakes. The earthquake source of these regions can be located in the continental shelf extending form the coastal land to offshore undersea, imposing extra hazards to offshore wind farms. Earthquake hazard is also known as seismic hazard, as earthquakes generally introduce seismic motions. A review on seismic hazard of wind turbines is documented in Ref. [144].

In order to develop safe and sustainable offshore wind farms, it is therefore crucial to develop advanced reliability assessment models taking into account multiple hazards. Evangelos et al. [145] assessed the structural performance of a 5 MW OWT subjected to multi-hazard environment, taking into account wind, wave and earthquake loads, through time domain analysis. The results indicated that the earthquake excitations can significantly affect the dynamic response of OWT towers and adversely affect the reliability of OWTs. Maryam and Paolo [146] developed a probabilistic framework to evaluate the structural reliability of OWT subjected to multiple hazards, considering earthquake ground motions and extreme wind conditions. The developed framework was applied to two identical OWTs deployed at two different locations, assessing their annual probabilities of failure. A widely used method for hazard analysis is the STPA (System-Theoretic Process Analysis) [147,148], which allows the exploration of hazardous scenarios caused by component failures. More efforts are required in the future to develop advanced reliability assessment models to take into account multiple hazards.

6.5. RBI (risk-based inspection)

Fig. 2 presents the main cost contributions of a typical offshore wind farm [149]. As can be seen from Fig. 2, the O&M (Operation and Maintenance) costs constitute about 28.2% of the total life-cycle cost of offshore wind farms. It can be also noted that the OWT support structures are among the most expensive components of offshore wind farms,

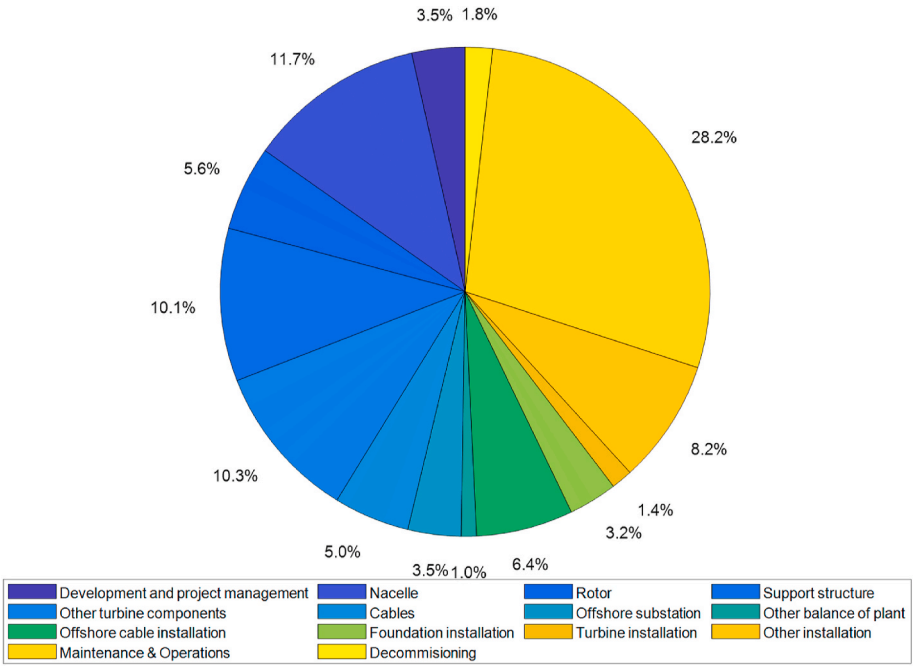

Fig. 2. The main cost contributions of a typical offshore wind farm (data source from Ref. [150]).

constituting around 10% of capital expenditures. Therefore, the development of cost-effective and well-planned inspection and maintenance methods for OWT support structures is crucial to reduce the total O&M and inspection costs.

RBI is the process of developing an inspection scheme considering the risk of failure. The fundamental process of RBI is a risk analysis, which combines a reliability analysis (i.e. evaluating the probability of failure) with an assessment of the consequences of failure. RBI has been widely applied to many industry sectors, such as Aerospace and Civil Engineering. It has been recently applied to the offshore wind industry.

Jose and John [151] applied RBI to jacket support structures of OWTs. The results demonstrated that the RBI is useful for optimising the inspection and maintenance activities to assure the achievement of a minimum reliability level. Papatzimos et al. [152] presented a RBI framework for offshore wind farms and applied it to the transition pieces of OWT support structures. Results indicated that the RBI can increase the safety of maintenance workers and lower the inspection costs by up to £0.7 million/MW installed. Mihai and John [153] presents a RBI strategy for offshore wind farms and applied it to a typical OWT blade. Results indicated that a reduction of 23% in annual maintenance expenses could be achieved with the use of RBI when compared to a traditional maintenance strategy. The application of RBI to the offshore wind industry is currently still limited to bottom-fixed OWTs, and studies on applying RSI to floating support structures would be seen in the future.

6.6. *Developing efficient reliability analysis methods*

Reliability analysis of OWT support structures generally involves highly nonlinear limit state functions and implicit finite element models, making it quite challenging and time-consuming to obtain precise results. Developing efficient reliability analysis methods, which reduce the computational time and at the same achieve reasonable accuracy, is important in the reliability-based design of OWT support structures.

Several studies have been performed to develop efficient reliability analysis methods. Sebastian et al. [154] developed an efficient reliability analysis method for OWT support structures based on an adaptive response surface method, and applied it to assess the reliability of a tripod support structure. Morató et al. [155] proposed an efficient reliability analysis method for OWT support structures based on the use of a Kriging model. The responses of the OWT support structure, which were obtained from stochastic fully coupled simulations in the time-domain, was approximated through the Kriging model. The reliability index was then computed using MCS. The method was applied to NREL 5 MW wind turbine on a monopile with a rigid foundation to assess its structural reliability. In their later work [156], the method was further applied to the NREL 5 MW wind turbine on a monopile with a flexible foundation. Teixeira et al. [157] proposed an efficient reliability assessment method based on density-scanned adaptive Kriging, and applied it to a complex function, a series system and a high dimensional engineering problem. The results indicated that the proposed method can improve the computational efficiency of reliability analysis. More studies on developing efficient reliability analysis methods for OWT support structures, especially the floating support structures, would be seen in the future.

7. Conclusions

OWT (Offshore Wind Turbine) support structures are exposed to harsh marine environment with significant uncertainties in soil properties and environmental loads. Traditional design method, which use PSFs (Partial Safety Factors) to consider uncertainties in uncertain variables, may lead to either over- or under-engineering the structure. Reliability-based design, which takes into account uncertainties accurately by modelling uncertain variables stochastically with appropriate types of distributions, is more suitable for future design of OWT support structures. Therefore, it is crucial to investigate the reliability of OWT support structure in order to develop more cost-effective OWT support structures.

This paper presents a comprehensive review on the reliability of OWT support structures, covering structural reliability, reliability-based calibration, fatigue reliability and the implementation of reliability assessment. The aspects to be considered more frequently in future reliability research of OWT support structures are also discussed.

SHM (Structural Health Modelling) and CM (Condition Monitoring) systems are now available at a lower cost, allowing collection of loading and loading effects as well as structural response data. Incorporating SHM/CM with reliability assessment allows the accurate update of

reliability index based on actual monitored data, providing valuable information for decision making on inspection and maintenance of OWT support structures. The monitored data obtained from SHM and CM systems are also valuable to quantify the characteristics of stochastic values.

Reliability assessment of OWT support structures provides valuable information for planning for maintenance. It can be integrated with the assessment of consequences of failure to develop RBI (Risk-Based Inspection), which is beneficial to reducing the maintenance cost of OWT support structures. Additionally, reliability assessment methods of OWT support structures can be further integrated with an optimiser (e.g. genetic algorithm) to perform RBDO (Reliability-Based Design Optimisation), optimising the OWT support structures to achieve target reliability index.

Declaration of competing interest

The authors declare that they have no known competing financial interests or personal relationships that could have appeared to influence the work reported in this paper.

References

[1] GWEC. Global wind report 2019. Brus-sels, Belgium: Global Wind Energy Council; 2020.
[2] Kaldellis J, Kapsali M. Shifting towards offshore wind energy—recent activity and future development. Energy Pol 2013;53:136–48.
[3] WindEurope. Offshore wind in Europe: key trends and statistics 2019. WindEurope; 2020.
[4] WindEurope. Wind energy in Europe: scenarios for 2030. 2017.
[5] Wiser R, Yang Z, Hand M, O H. Wind energy. In: Edenhofer O, et al., editors. IPCC special report on renewable energy sources and climate Change mitigation. Cambridge: Cambridge University Press; 2011.
[6] Esteban M, Couñago B, López-Gutiérrez J, Negro V, Vellisco F. Gravity based support structures for offshore wind turbine generators: review of the installation process. Ocean Eng 2015;110:281–91.
[7] Yeter B, Garbatov Y, Soares CG. Uncertainty analysis of soil-pile interactions of monopile offshore wind turbine support structures. Appl Ocean Res 2019;82:74–88.
[8] Yeter B, Tekgoz M, Garbatov Y, Soares CG. Fragility analysis of an ageing monopile offshore wind turbine subjected to simultaneous wind and seismic load. Safety in Extreme Environments 2020:1–16.
[9] Houlsby GT, Byrne BW. Suction caisson foundations for offshore wind turbines and anemometer masts. Wind Eng 2000;24:249–55.
[10] Wang H, Cheng X. Undrained bearing capacity of suction caissons for offshore wind turbine foundations by numerical limit analysis. Mar Georesour Geotechnol 2016;34:252–64.
[11] Yeter B, Garbatov Y, Guedes Soares C. Ultimate strength assessment of jacket offshore wind turbine support structures subjected to progressive bending loading. Ships Offshore Struct 2019;14:165–75.
[12] Ju S-H, Su F-C, Ke Y-P, Xie M-H. Fatigue design of offshore wind turbine jacket-type structures using a parallel scheme. Renew Energy 2019;136:69–78.
[13] Mazarakos TP, Mavrakos SA, Soukisian TH. Wave loading and wind energy of a spar buoy floating wind turbine. In: 2019 fourteenth international conference on ecological vehicles and renewable energies (EVER). IEEE; 2019. p. 1–7.
[14] Tomasicchio GR, D'Alessandro F, Avossa AM, Riefolo L, Musci E, Ricciardelli F, et al. Experimental modelling of the dynamic behaviour of a spar buoy wind turbine. Renew Energy 2018;127:412–32.
[15] Zhang M, Li X, Xu J. Smart control of fatigue loads on a floating wind turbine with a tension-leg-platform. Renew Energy 2019;134:745–56.
[16] Han Y, Le C, Ding H, Cheng Z, Zhang P. Stability and dynamic response analysis of a submerged tension leg platform for offshore wind turbines. Ocean Eng 2017;129:68–82.
[17] Xie S, Jin X, He J, Zhang C. Structural responses suppression for a barge-type floating wind turbine with a platform-based TMD. IET Renew Power Gener 2019;13:2473–9.
[18] Wu X, Hu Y, Li Y, Yang J, Duan L, Wang T, et al. Foundations of offshore wind turbines: a review. Renew Sustain Energy Rev 2019;104:379–93.
[19] Igwemezie V, Mehmanparast A, Kolios A. Current trend in offshore wind energy sector and material requirements for fatigue resistance improvement in large wind turbine support structures–A review. Renew Sustain Energy Rev 2019;101:181–96.
[20] Asheghabadi MS, Sahafnia M, Bahadori A, Bakhshayeshi N. Seismic behavior of suction caisson for offshore wind turbine to generate more renewable energy. Int J Environ Sci Technol 2019;16:2961–72.
[21] Kolios A, Mytilinou V, Lozano-Minguez E, Salonitis K. A comparative study of multiple-criteria decision-making methods under stochastic inputs. Energies 2016;9:566.
[22] Kolios A, Wang L, Mehmanparast A, Brennan F. Determination of stress concentration factors in offshore wind welded structures through a hybrid experimental and numerical approach. Ocean Eng 2019;178:38–47.
[23] JrH Thomsen, Forsberg T, Bittner R. Offshore wind turbine foundation: the COWI experience. In: International conference on offshore mechanics and arctic engineering; 2007. p. 533–40.
[24] Seidel M. Feasibility of monopiles for large offshore wind turbines. In: Proceedings of the 10th German wind energy conference (DEWEK) REpower systems AG; 2010.
[25] Hermans K, Peeringa J. Future XL monopile foundation design for a 10 MW wind turbine in deep water. ECN; 2016.
[26] Pein T, Foglia A, Kayen R, Moerz T. Comparison of laboratory and in-situ small strain soil stiffness for modelling lateral bearing capacities of XL monopiles. In: The 28th international ocean and polar engineering conference. International Society of Offshore and Polar Engineers; 2018.
[27] Tripods. Jackets and tripiles: innovative tube systems for offshore wind energy systems. https://www.tube-tradefair.com/en/Press/Press_material/Archive_Press_releases_for_Tube/FA_09_Tripods,_Jackets_and_Tripiles_Innovative_Tube_Systems_for_Offshore_Wind_Energy_Systems. [Accessed 5 November 2020].
[28] Shi W, Park HC, Chung CW, Shin HK, Kim SH, Lee SS, et al. Soil-structure interaction on the response of jacket-type offshore wind turbine. International Journal of Precision Engineering and Manufacturing-Green Technology 2015;2:139–48.
[29] Natarajan A, Stolpe M, Wandji WN. Structural optimization based design of jacket type sub-structures for 10 MW offshore wind turbines. Ocean Eng 2019;172:629–40.
[30] Bachynski EE. Fixed and floating offshore wind turbine support structures. Offshore Wind Energy Technology; 2018. p. 103.
[31] Bento N, Fontes M. Emergence of floating offshore wind energy: technology and industry. Renew Sustain Energy Rev 2019;99:66–82.
[32] Liu Y, Li S, Yi Q, Chen D. Developments in semi-submersible floating foundations supporting wind turbines: a comprehensive review. Renew Sustain Energy Rev 2016;60:433–49.
[33] Cho S, Bachynski EE, Nejad AR, Gao Z, Moan T. Numerical modeling of the hydraulic blade pitch actuator in a spar-type floating wind turbine considering fault conditions and their effects on global dynamic responses. Wind Energy; 2019.
[34] Kolios A, Di Maio LF, Wang L, Cui L, Sheng Q. Reliability assessment of point-absorber wave energy converters. Ocean Eng 2018;163:40–50.
[35] Schubert M, Lind MT, Eriksson M, Jacobsen F. Reliability assessment of an existing offshore steel structure with hot spots. Int J Offshore Polar Eng 2017;27:433–41.
[36] Abaei MM, Abbassi R, Garaniya V, Chai S, Khan F. Reliability assessment of marine floating structures using Bayesian network. Appl Ocean Res 2018;76:51–60.
[37] Yeter B, Garbatov Y, Soares CG. System reliability of a jacket offshore wind turbine subjected to fatigue. Progress in the Analysis and Design of Marine Structures. London, UK: Taylor & Francis Group; 2017.
[38] Standardization ECf. Eurocode 3: design of steel structures. CEN; 1992.
[39] Mazzolani F. Background document of EUROCODE 8. In: Proceedings of the first state of the art Workshop,"Semi-rigid behaviour of civil engineering structural connections"-COST C. chapter 3: Steel Structures 1992. p. 28–30.
[40] Mazzolani F. Eurocode 8-chapter "Steel": background and remarks. In: Proceedings of 10th European conference on earthquake engineering. ECEE; 1995.
[41] Scheu MN, Tremps L, Smolka U, Kolios A, Brennan F. A systematic Failure Mode Effects and Criticality Analysis for offshore wind turbine systems towards integrated condition based maintenance strategies. Ocean Eng 2019;176:118–33.
[42] Martinez-Luengo M, Shafiee M. Guidelines and cost-benefit analysis of the structural health monitoring implementation in offshore wind turbine support structures. Energies 2019;12:1176.
[43] Yeter B, Garbatov Y, Soares CG. Fatigue reliability of an offshore wind turbine supporting structure accounting for inspection and repair. Analysis and Design of Marine Structures V. CRC Press; 2015. p. 751–62.
[44] Dong P, Hong JK, Osage DA, Prager M. Master SN curve method for fatigue evaluation of welded components. Welding Research Council Bulletin; 2002.
[45] Anderson TL. Fracture mechanics: fundamentals and applications. CRC press; 2017.
[46] Sheng SS. Report on wind turbine subsystem Reliability— A survey of various databases. 2013.
[47] Wen J, Zheng Y, Donghan F. A review on reliability assessment for wind power. Renew Sustain Energy Rev 2009;13:2485–94.
[48] Pfaffel S, Faulstich S, Rohrig K. Performance and reliability of wind turbines: a review. Energies 2017;10:1904.
[49] Agarwal P. Structural reliability of offshore wind turbines. 2008.
[50] Classification DNV. Notes No. 30.6: structural reliability analysis of marine structures. DNV; 1992.
[51] Wong FS. First-order, second-moment methods. Comput Struct 1985;20:779–91.
[52] Gollwitzer S, Abdo T, Rackwitz R. First order reliability method (FORM) manual. Nymphenburger Str: RCP Gmbh; 1988. p. 134.
[53] Der Kiureghian A, Lin H-Z, Hwang S-J. Second-order reliability approximations. J Eng Mech 1987;113:1208–25.
[54] Earl DJ, Deem MW. Monte Carlo simulations. Molecular modeling of proteins. Springer; 2008. p. 25–36.
[55] Kim DH, Lee SG. Reliability analysis of offshore wind turbine support structures under extreme ocean environmental loads. Renew Energy 2015;79:161–6.

[56] Peeringa J, Bedon G. Fully integrated load analysis included in the structural reliability assessment of a monopile supported offshore wind turbine. Energy Proc 2017;137:255–60.
[57] Api. 2A-LRFD: API recommended practices for planning, designing and constructing fixed offshore platforms–load and resistance factor design. July; 1993.
[58] API. API recommended practice 2A-WSD for planning, designing, and constructing fixed offshore platforms - working stress design. American Petroleum Institute; 2014.
[59] CEN. Eurocode 1990:2002 Basis of structural design EU. CEN; 2002.
[60] B1. The EUROCODES: implimentation and use. EU; 2008.
[61] CEN. BS EN 1993-1-1:2005+a1:2014 Eurocode 3: design of steel structures. CEN; 2015.
[62] IEC. IEC 61400-3-1:2019: wind energy generation systems - Part 3-1: design requirements for fixed offshore wind turbines. International Electrotechnical Commission 2019.
[63] IEC. IEC 61400-3-2:2019: wind energy generation systems - Part 3-2: design requirements for floating offshore wind turbines. International Electrotechnical Commission 2019.
[64] IEC. IEC 61400-1:2019: wind energy generation systems - Part 1: design requirements. International Electrotechnical Commission 2019.
[65] DNVGL. DNVGL-ST-0126: support structures for wind turbines. DNVGL; 2016.
[66] DNVGL. DNVGL-ST-0119: floating wind turbine structures. DNVGL; 2018.
[67] DNVGL. DNVGL-ST-0145: offshore substations. DNVGL; 2016.
[68] ABS. Guide for building and classing bottom-founded offshore wind turbine installations. ABS; 2013.
[69] ABS. Guide for building and classing floating offshore wind turbine installations. ABS; 2013.
[70] Veritas B. NI572 - classification and certification of floating offshore wind turbines. Veritas Bureau; 2019.
[71] Veritas B. NR445 - rules for the classification of offshore units. Veritas Bureau; 2016.
[72] Veritas B. NI631 - certification scheme for marine renewable energy technologies. Veritas Bureau; 2016.
[73] Iso E. ISO 19902/A1:2015: Petroleum and natural gas industries – fixed steel offshore structures EN ISO. 2015.
[74] Bhattacharya B, Basu R, Ma K-t. Developing target reliability for novel structures: the case of the Mobile Offshore Base. Mar Struct 2001;14:37–58.
[75] ISO. ISO 2394 - general principles on reliability for structures. ISO; 1998.
[76] Sørensen JD. Reliability-based calibration of fatigue safety factors for offshore wind turbines. In: The twenty-first international offshore and polar engineering conference. OnePetro; 2011.
[77] Velarde J, Mankar A, Kramhøft C, Sørensen JDJES. Probabilistic calibration of fatigue safety factors for offshore wind turbine concrete structures, vol. 222; 2020. p. 111090.
[78] Morató A, Sriramula SJMS. Calibration of safety factors for offshore wind turbine support structures using fully coupled simulations, vol. 75; 2021. p. 102880.
[79] Kolios A, Brennan F. Reliability based design for novel offshore structures. In: The proceedings of the 3rd international conference of integrity. Porto: Reliability and Failure; 2009.
[80] Morató A, Sriramula S. Calibration of safety factors for offshore wind turbine support structures using fully coupled simulations. Mar Struct 2021;75:102880.
[81] Dong W, Moan T, Gao Z. Fatigue reliability analysis of the jacket support structure for offshore wind turbine considering the effect of corrosion and inspection. Reliab Eng Syst Saf 2012;106:11–27.
[82] Van Vuong N, Quan MH. Fatigue analysis of jacket support structure for offshore wind turbines. Journal of Science and Technology in Civil Engineering (STCE)-NUCE 2019;13:46–59.
[83] Chian C-Y, Zhao Y-Q, Lin T-Y, Nelson B, Huang H-H. Comparative study of time-domain fatigue assessments for an offshore wind turbine jacket substructure by using conventional grid-based and Monte Carlo sampling methods. Energies 2018;11:3112.
[84] Ayyub BM, Assakkaf IA, Kihl DP, Siev MW. JNej. Reliability-based design guidelines for fatigue of ship structures, vol. 114; 2002. p. 113–38.
[85] Adedipe O, Brennan F, Kolios A. Review of corrosion fatigue in offshore structures: present status and challenges in the offshore wind sector. Renew Sustain Energy Rev 2016;61:141–54.
[86] Broek D. Elementary engineering fracture mechanics. Springer Science & Business Media; 2012.
[87] Chen H-Y, Lin T-H, Li P-K. Fast design of jerusalem-cross parameters by equivalent circuit model and least-square curve fitting technique. Appl Comput Electromagn Soc J 2015;30.
[88] Lauritzen S, Uhler C, Zwiernik P. Maximum likelihood estimation in Gaussian models under total positivity. Ann Stat 2019;47:1835–63.
[89] Raqab MZ, Alkhalfan LA, Bdair OM, Balakrishnan N. Maximum likelihood prediction of records from 3-parameter Weibull distribution and some approximations. J Comput Appl Math 2019;356:118–32.
[90] DNVGL. DNVGL-RP-C203: fatigue design of offshore steel structures. DNVGL; 2016.
[91] Sørum SH, Krokstad JR, Amdahl J. Wind-wave directional effects on fatigue of bottom-fixed offshore wind turbine. In: Journal of physics: conference series. IOP Publishing; 2019. p. 12011.
[92] Wilberts F. Measurement driven fatigue assessment OF offshore wind turbine foundations. 2017.
[93] Mehmanparast A, Brennan F, Tavares I. Fatigue crack growth rates for offshore wind monopile weldments in air and seawater: SLIC inter-laboratory test results. Mater Des 2017;114:494–504.
[94] Miner M. Cumulative fatigue damage. J Appl Mech 1945;12:A159–64.
[95] Karim MR, Islam MA. Reliability and survival analysis. Springer; 2019.
[96] Najem Clarke S, Goodpasture DW, Bennett RM, Deatherage JH, Burdette EG. Effect of cycle-counting methods on effective stress range and number of stress cycles for fatigue-prone details. Transport Res Rec 2000;1740:49–60.
[97] Socie D. Rainflow cycle counting: a historical perspective. The Rainflow Method in Fatigue. Elsevier; 1992. p. 3–10.
[98] Marsh G, Wignall C, Thies PR, Barltrop N, Incecik A, Venugopal V, et al. Review and application of Rainflow residue processing techniques for accurate fatigue damage estimation. Int J Fatig 2016;82:757–65.
[99] Li H, Hu Z, Wang J, Meng X. Short-term fatigue analysis for tower base of a spar-type wind turbine under stochastic wind-wave loads. International Journal of Naval Architecture and Ocean Engineering 2018;10:9–20.
[100] Yeter B, Garbatov Y, Soares CG. Fatigue damage assessment of fixed offshore wind turbine tripod support structures. Eng Struct 2015;101:518–28.
[101] Han C, Ma Y, Qu X, Qin P, Qiu B. A fast and practical method for predicting the fatigue life of offshore wind turbine jacket support structures. In: International conference on offshore mechanics and arctic engineering. American Society of Mechanical Engineers; 2017. p. V010T09A43.
[102] Velarde J, Kramhøft C, Sørensen JD, Zorzi G. Fatigue reliability of large monopiles for offshore wind turbines. Int J Fatig 2020;134:105487.
[103] Colone L, Natarajan A, Dimitrov N. Impact of turbulence induced loads and wave kinematic models on fatigue reliability estimates of offshore wind turbine monopiles. Ocean Eng 2018;155:295–309.
[104] Horn J-T, Leira BJ. Fatigue reliability assessment of offshore wind turbines with stochastic availability. Reliab Eng Syst Saf 2019;191:106550.
[105] Shittu AA, Mehmanparast A, Shafiee M, Kolios A, Hart P, Pilario K. Structural reliability assessment of offshore wind turbine support structures subjected to pitting corrosion-fatigue: a damage tolerance modelling approach. Wind Energy 2020;23:2004–26.
[106] Wang L, Kolios A. A generic framework for reliability assessment of offshore wind turbine monopiles. In: 6th international conference on marine structures (MARSTRUCT 2017). Lisbon, Portugal; 2017.
[107] Bhattacharya S. Challenges in design of foundations for offshore wind turbines. Engineering & Technology Reference 2014;1:922.
[108] Kallehave D, Byrne BW, LeBlanc Thilsted C, Mikkelsen KK. Optimization of monopiles for offshore wind turbines. Phil Trans Math Phys Eng Sci 2015;373:20140100.
[109] Gentils T, Wang L, Kolios A. Integrated structural optimisation of offshore wind turbine support structures based on finite element analysis and genetic algorithm. Appl Energy 2017;199:187–204.
[110] Wang L, Kolios A, Nishino T, Delafin P-L, Bird T. Structural optimisation of vertical-axis wind turbine composite blades based on finite element analysis and genetic algorithm. Compos Struct 2016;153:123–38.
[111] Carswell W, Arwade SR, DeGroot DJ, Lackner MA. Soil–structure reliability of offshore wind turbine monopile foundations. Wind Energy 2015;18:483–98.
[112] Drucker DC, Prager W. Soil mechanics and plastic analysis or limit design. Q Appl Math 1952;10:157–65.
[113] Labuz JF, Zang A. Mohr–Coulomb failure criterion. Rock Mech Rock Eng 2012;45:975–9.
[114] Byrne B, McAdam R, Burd H, Houlsby G, Martin C, Beuckelaers W, et al. PISA: new design methods for offshore wind turbine monopiles. 2017.
[115] Byrne BW, Burd HJ, Zdravković L, McAdam RA, Taborda DM, Houlsby GT, et al. PISA: new design methods for offshore wind turbine monopiles. Rev Fr Geotech 2019;3.
[116] Byrne BW, Burd HJ, Zdravkovic L, Abadie CN, Houlsby GT, Jardine RJ, et al. PISA design methods for offshore wind turbine monopiles. In: Offshore technology conference. Offshore Technology Conference; 2019.
[117] Byrne BW, Houlsby GT, Burd HJ, Gavin KG, Igoe DJ, Jardine RJ, et al. PISA design model for monopiles for offshore wind turbines: application to a stiff glacial clay till. Geotechnique 2020:1–18.
[118] Schauer M, Taddei F, Rodriguez GAR. Seismic transient simulation of an operating wind turbine considering the soil-structure interaction. In: Journal of physics: conference series. IOP Publishing; 2019. p. 12022.
[119] Zdravković L, Taborda DM, Potts DM, Abadias D, Burd HJ, Byrne BW, et al. Finite-element modelling of laterally loaded piles in a stiff glacial clay till at Cowden. Geotechnique 2019:1–15.
[120] Pisanò F, Schipper R, Schreppers G-J. Input of fully 3D FE soil-structure modelling to the operational analysis of jack-up structures. Mar Struct 2019;63:269–88.
[121] Abhinav K, Saha N. Effect of scouring in sand on monopile-supported offshore wind turbines. Mar Georesour Geotechnol 2017;35:817–28.
[122] Ma H, Yang J, Chen L. Effect of scour on the structural response of an offshore wind turbine supported on tripod foundation. Appl Ocean Res 2018;73:179–89.
[123] Van der Tempel J, Zaaijer M, Subroto H. The effects of scour on the design of offshore wind turbines. In: Proceedings of MAREC; 2004.
[124] Rezaei R, Duffour P, Fromme P. Scour influence on the fatigue life of operational monopile-supported offshore wind turbines. Wind Energy 2018;21:683–96.
[125] Velarde J, Kramhøft C, Sørensen JD. Uncertainty modeling and fatigue reliability assessment of concrete gravity based foundation for offshore wind turbines. In: The 28th international ocean and polar engineering conference. International Society of Offshore and Polar Engineers; 2018.

[126] Vahdatirad MJ, Griffiths D, Andersen LV, Sørensen JD, Fenton G. Reliability analysis of a gravity-based foundation for wind turbines: a code-based design assessment. Geotechnique 2014;64:635–45.
[127] Okpokparoro S, Sriramula S. Uncertainty modeling in reliability analysis of floating wind turbine support structures. Renew Energy 2021;165:88–108.
[128] Martinez-Luengo M, Kolios A, Wang L. Structural health monitoring of offshore wind turbines: a review through the Statistical Pattern Recognition Paradigm. Renew Sustain Energy Rev 2016;64:91–105.
[129] Lian J, Cai O, Dong X, Jiang Q, Zhao Y. Health monitoring and safety evaluation of the offshore wind turbine structure: a review and discussion of future development. Sustainability 2019;11:494.
[130] Lee Y-J, Cho S. SHM-based probabilistic fatigue life prediction for bridges based on FE model updating. Sensors 2016;16:317.
[131] Li H, Li S, Ou J, Li H. Reliability assessment of cable-stayed bridges based on structural health monitoring techniques. Structure and Infrastructure Engineering 2012;8:829–45.
[132] Kolios A, Wang L. Advanced reliability assessment of offshore wind turbine monopiles by combining reliability analysis method and SHM/CM technology. In: The 28th international ocean and polar engineering conference. International Society of Offshore and Polar Engineers; 2018.
[133] Johansen SS, Nejad AR. On digital twin condition monitoring approach for drivetrains in marine applications. In: International conference on offshore mechanics and arctic engineering. American Society of Mechanical Engineers; 2019. p. V010T09A3.
[134] Martinez-Luengo M, Shafiee M, Kolios A. Data management for structural integrity assessment of offshore wind turbine support structures: data cleansing and missing data imputation. Ocean Eng 2019;173:867–83.
[135] Kubat M. Artificial neural networks. An introduction to machine learning. Springer; 2021. p. 117–43.
[136] Suthaharan S. Support vector machine. Machine learning models and algorithms for big data classification. Springer; 2016. p. 207–35.
[137] Lee Y-S, Choi B-L, Lee JH, Kim SY, Han S. Reliability-based design optimization of monopile transition piece for offshore wind turbine system. Renew Energy 2014; 71:729–41.
[138] Yang H, Zhu Y, Lu Q, Zhang J. Dynamic reliability based design optimization of the tripod sub-structure of offshore wind turbines. Renew Energy 2015;78:16–25.
[139] Stieng LES, Muskulus M. Reliability-based design optimization of offshore wind turbine support structures using analytical sensitivities and factorized uncertainty modeling. 2020.
[140] Velarde J, Kramhøft C, Sørensen JD. Reliability-based design optimization of offshore wind turbine concrete structures. 2019.
[141] Yang H, Zhang X, Xiao F. Dynamic reliability based design optimization of offshore wind turbines considering uncertainties. In: The thirteenth ISOPE pacific/asia offshore mechanics symposium. International Society of Offshore and Polar Engineers; 2018.
[142] Khalafallah MG, Ahmed AM, Emam MK. JAiME. The effect of using winglets to enhance the performance of swept blades of a horizontal axis wind turbine, vol. 11; 2019. 1687814019878312.
[143] Chen X, Li C, Tang J. Structural integrity of wind turbines impacted by tropical cyclones: a case study from China. In: Journal of physics: conference series. IOP Publishing; 2016. p. 42003.
[144] Katsanos EI, Thöns S, Georgakis CT. Wind turbines and seismic hazard: a state of the art review. Wind Energy 2016;19:2113–33.
[145] Katsanos EI, Sanz AA, Georgakis CT, Thöns S. Multi-hazard response analysis of a 5MW offshore wind turbine. Procedia Eng 2017;199:3206–11.
[146] Mardfekri M, Gardoni P. Multi-hazard reliability assessment of offshore wind turbines. Wind Energy 2015;18:1433–50.
[147] Puisa R, Bolbot V, Newman A, Vassalos D. Systemic hazard analysis of offshore service operations. Wind Energy Science Discussions; 2020. p. 1–20.
[148] Abrecht B, Leveson N. Systems theoretic process analysis (STPA) of an offshore supply vessel dynamic positioning system. Cambridge, MA: Massachusetts Institute of Technology; 2016.
[149] Musial W, Ram B. Large-scale offshore wind power in the United States: assessment of opportunities and barriers. Golden, CO (United States): National Renewable Energy Lab.(NREL); 2010.
[150] Wind farm costs. https://guidetoanoffshorewindfarm.com/wind-farm-costs. [Accessed 3 October 2020].
[151] Rangel-Ramírez JG, Sørensen JD. Risk-based inspection planning optimisation of offshore wind turbines. Structure and Infrastructure Engineering 2012;8:473–81.
[152] Papatzimos AK, Dawood T, Thies P. Cost-effective risk-based inspection planning for offshore wind farms. Insight-Non-Destructive Testing and Condition Monitoring 2018;60:299–305.
[153] Florian M, Sørensen JD. Risk-based planning of operation and maintenance for offshore wind farms. Energy Proc 2017;137:261–72.
[154] Thons S, Faber MH, Rucker W. Support structure reliability of offshore wind turbines utilizing an adaptive response surface method. In: International conference on offshore mechanics and arctic engineering; 2010. p. 407–16.
[155] Morató A, Sriramula S, Krishnan N. Reliability analysis of offshore wind turbine support structures using kriging models. In: Walls L, Revie M, Bedford B, editors. Risk, reliability and safety: innovating theory and practice; 2016.
[156] Morató A, Sriramula S, Krishnan N. Kriging models for aero-elastic simulations and reliability analysis of offshore wind turbine support structures. Ships Offshore Struct 2019;14:545–58.
[157] Teixeira R, Nogal M, O'Connor A, Martinez-Pastor B. Reliability assessment with density scanned adaptive Kriging. Reliability Engineering & System Safety; 2020. p. 106908.